IMMUNOLOGY

Eosinophilic inflammation promotes CCL6-dependent metastatic tumor growth

Fei Li[1†], Xufei Du[1†], Fen Lan[1†], Na Li[1†], Chao Zhang[1], Chen Zhu[1], Xiaohui Wang[1], Yicheng He[1], Zhehua Shao[1], Haixia Chen[1], Man Luo[1], Wen Li[1], Zhihua Chen[1], Songmin Ying[1,2,3]*, Huahao Shen[1,4]*

Compelling evidence suggests that inflammatory components contribute to cancer development. However, eosinophils, involved in several inflammatory diseases, were not fully explored in cancer metastasis. We show that airway inflammatory eosinophilia and colonic inflammation with eosinophil infiltration are both associated with increased metastasis in mice. Eosinophilia is responsible for increased bone metastasis in eosinophil-enriched *Cd3δ-Il-5* transgenic (*Il-5* Tg) mice. We also observe increased eosinophils in the malignant pleural effusion of cancer patients with pleural metastasis. Mechanistically, eosinophils promote tumor cell migration and metastasis formation through secreting C-C motif chemokine ligand 6 (CCL6). Genetic knockout of *Ccl6* in *Il-5* Tg mice remarkably attenuates bone metastasis. Moreover, inhibition of C-C chemokine receptor 1 (CCR1, the receptor of CCL6) in tumor cells reduces tumor cell migration and metastasis. Thus, our study identifies a CCL6-dependent prometastatic activity of eosinophils, which can be inhibited by targeting CCR1 and represent an approach to preventing metastatic disease.

INTRODUCTION

Compelling evidence supports the involvement of inflammatory components in different stages of cancer development, including carcinogenesis, cancer invasion, and metastasis (*1*). However, allergen-induced airway inflammation, marked by notable infiltration of eosinophils into inflammatory sites, has been reported to have an inverse cancer risk association in epidemiological and experimental studies (*2*). Eosinophil infiltration is also frequently observed in various solid tumors in the clinic and is usually associated with a favorable prognosis in most studies (*3*), indicating that eosinophils play a potential antitumor role. This triggered a wealth of research addressing the underlying mechanisms involved. Several studies have demonstrated the antitumor function of eosinophils both in vivo and in vitro (*4*–*6*) and have highlighted various mechanisms, summarized as (i) degranulation of cytotoxic granules and enzymes to directly kill the tumor cells, and (ii) production of a wide range of immunologically active factors to modulate tumor environment (*7*). However, there is little information available about the direct effects of eosinophils on tumor metastasis.

Eosinophilic inflammation within the tumor microenvironment can also enable the establishment of metastasis (*8*). Eosinophil-related cytokines, such as interleukin-5 (IL-5), are pivotal factors that contribute to the differentiation and survival of eosinophils in allergic inflammation. Although confounding factors complicate the relationship between eosinophilic inflammation and tumor (*9*), it has been documented that IL-5 determines metastatic colonization of the lung through eosinophils (*10*). Eosinophil peroxidase (EPX) has been reported to facilitate tumor metastasis in a 4T1 breast cancer model (*11*). Determined upon tissue staining, EPX has also been identified as a potential biomarker to predict the clinical outcome of patients with primary lung adenocarcinoma (*12*). These studies have shown that eosinophils and their mediators may play a much greater role in cancer metastasis than previously understood. Thus, the antitumor role of eosinophils should be reconsidered until there are more evidence and functional mechanisms about eosinophils in cancer metastasis.

C-C chemokine ligand 6 (CCL6) is a chemokine previously reported to be mainly produced in monocytes or macrophages (*13*), whereas our previous study showed CCL6 production by eosinophils in allergic airway inflammation (*14*). Overexpression of CCL6 can accelerate tumor growth as well as enhance local and metastatic spread in mice (*15*). CCL6 shares homology with the human C-C chemokine, MPIF-1/CCL23 (*16*), which has been significantly up-regulated in tumor tissues (*17*). High expression of CCL23 is correlated with the accelerated progression and the short survival of patients with cancer (*18*). Previous studies have demonstrated that CCL6/CCL23 binds to and activates C-C chemokine receptor 1 (CCR1), expressed on the surface of a variety of immune cells and tumor cells to promote tumor metastasis (*19*, *20*). Here, we hypothesized that CCL6-CCR1 signaling would be involved in eosinophil-associated cancer metastasis. Thus, we investigated the function of eosinophils in the context of inflammation on experimental tumor cell metastasis and found that eosinophils promote CCL6-dependent metastatic tumor growth.

RESULTS

Ovalbumin-induced airway inflammation and dextran sulfate sodium–induced colonic inflammation promote metastasis in mice

To determine the effect of inflammation accompanied by eosinophilia on tumor metastasis, we first established a melanoma model of lung metastasis (*21*) following the classic ovalbumin (OVA)–induced asthma model (*22*) in C57BL/6 wild-type (WT) mice

[1]Key Laboratory of Respiratory Disease of Zhejiang Province, Department of Respiratory and Critical Care Medicine, The Second Affiliated Hospital of Zhejiang University School of Medicine, Hangzhou, Zhejiang 310009, China. [2]International Institutes of Medicine, The Fourth Affiliated Hospital of Zhejiang University School of Medicine, Yiwu 322000, China. [3]Department of Pharmacology, Zhejiang University School of Medicine, Hangzhou 310058, China. [4]State Key Lab of Respiratory Disease, Guangzhou 510120, China.
*Corresponding author. Email: huahaoshen@zju.edu.cn (H.S.); yings@zju.edu.cn (S.Y.)
†These authors contributed equally to this work.

(Fig. 1A). We observed significantly increased lung metastasis in the mice with airway inflammation, compared with that in control mice (Fig. 1, B and C). An experimental dextran sulfate sodium (DSS)–induced colitis model was then established, followed by tumor cell injection into the abdominal cavities (*23*) (Fig. 1D). Also, DSS-induced colonic inflammation resulted in an aggravating phenotype in colon metastasis (Fig. 1, E and F). We subsequently explore the effect of relieving the inflammation to prevent metastasis. A wide-spectrum anti-inflammatory agent, dexamethasone (DEX), effectively inhibited airway inflammation to reduce lung metastasis (Fig. 1, G to I).

To confirm the eosinophilia, we performed immunohistochemistry and flow cytometry analysis of lung tissue in the OVA model and colons in the DSS model. As expected, the results identified eosinophil infiltration in the airway inflammation (fig. S1, A and B). DSS-induced colitis presented abundant infiltration of leukocytes in colonic mucosa including eosinophils (fig. S1, C and D). Notably, eosinophil-deficient (Eos-null) mice attenuated the lung metastasis following OVA challenge, whereas they exhibited no effects on the colon metastasis following DSS treatment (fig. S1, E and F). It was in line with the evidence that eosinophil deficiency abolishes OVA-induced airway inflammation but fails to relieve DSS-induced colitis (*24*, *25*).

Eosinophilia is indispensable for increased bone metastasis in *Cd3δ-Il-5* transgenic mice

Next, to investigate the long-term effects of persistent eosinophilia on metastasis in vivo, we took advantage of the *Cd3δ-Il-5* transgenic (*Il-5* Tg) mice in which a very high level of eosinophils is produced in the bone marrow (BM) and maintained in peripheral blood (*26*), as shown in Fig. 2A. Injection of tumor cells via caudal arteries delivers tumor cells to the organs downstream of the common iliac artery and predominantly develops bone metastasis in the lower

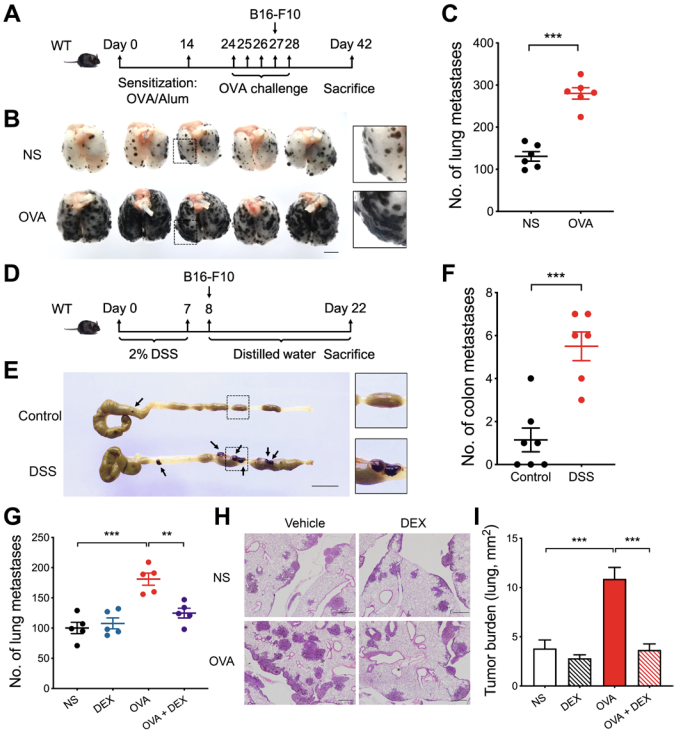

Fig. 1. Airway inflammation and colonic inflammation promotes metastasis. (**A**) Schematic timeline representing the merger of an established model of allergic airway inflammation and the metastasis of circulating B16-F10 cells to the lung. (**B**) Representative photograph of pulmonary metastatic foci on day 42. Scale bar, 5 mm. (**C**) The number of experimental pulmonary metastases. (**D**) Schematic timeline representing the merger of an established model of colitis and the metastasis of abdominal B16-F10 cells to the colon. (**E**) Representative photograph of colonic metastatic foci produced after injection of B16-F10 cells on day 22. Scale bar, 1 cm. (**F**) The number of colon metastases. (**G**) The number of experimental pulmonary metastases from mice treated with NS, dexamethasone (DEX), OVA, and OVA and DEX (OVA + DEX), respectively. (**H**) Representative lung hematoxylin and eosin section of metastases. Scale bars, 500 μm. (**I**) Quantification of the tumor burden per lung (mm^2) in (H). (C, F, G, and I) $n = 5$ to 7 mice per group. Statistical analyses were performed by Student's t test (C and F) and one-way ANOVA (G and I). Data are presented as mean ± SEM from one representative experiment of three independent experiments. $^{**}P < 0.01$; $^{***}P < 0.001$.

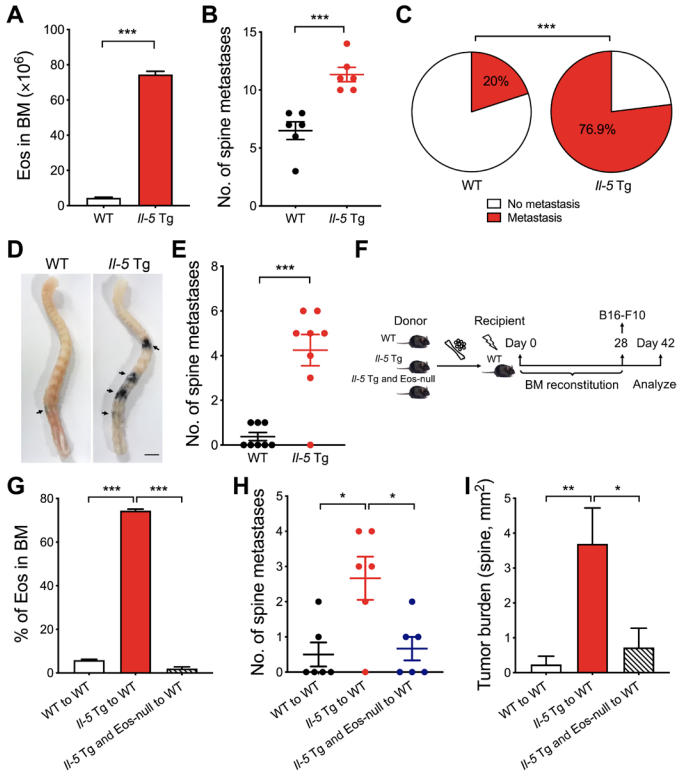

Fig. 2. Eosinophilia mediates enhanced bone metastasis in *Il-5* Tg mice. (**A**) The number of eosinophils in BM of WT and *Il-5* Tg mice, $n = 4$ mice per group. (**B**) Comparison of metastasis foci of spines on day 14. WT and *Il-5* Tg mice were injected with B16-F10 cells via caudal arteries. (**C**) The proportion of metastasis in the spine from mice injected with B16-F10 intravenously (WT, $n = 20$; *Il-5* Tg, $n = 26$). (**D**) Representative photograph of metastatic foci in the spine of WT and *Il-5* Tg mice injected with B16-F10 intravenously on day 14. (**E**) The number of the spine metastasis in (D). (**F**) Schematic representation of BM transplantation followed by establishing a metastasis model. (**G**) Frequencies of eosinophils in BM of WT mice that have received donor BM transplants from WT, *Il-5* Tg, or *Il-5* Tg and Eos-null mice 28 days ago. (**H**) Comparison of the metastatic foci in the spine on day 42. (**I**) Quantification of the tumor burden per area (mm^2) in the spine on day 42. (B, E, and G to I) $n = 6$ to 8 mice per group. Statistical analyses were performed by Student's t test (A, B, and E), one-way ANOVA (G, H, and I), and Fisher's exact test (C). Data (mean ± SEM) are from one representative experiment of three independent experiments. $^{*}P < 0.05$, $^{**}P < 0.01$, and $^{***}P < 0.001$.

spine and hindlimbs at high frequency (*27*). In contrast to fewer spine metastases in WT mice, we observed a greater number of visible pigmented spine lesions in *Il-5* Tg mice (Fig. 2B). Intravenous tail vein injection of tumor cells is reported to infrequently result in bone metastasis (*28*) (fig. S2A). However, the risk of metastasis was significantly higher in *Il-5* Tg mice, in addition to greater spine metastasis numbers (Fig. 2, C to E). Similar results were confirmed in the tibia and femur (fig. S2, B and C). Histological examination of the femur displayed an early stage of colonization and apparent tumor foci in *Il-5* Tg mice (fig. S2D).

Given that IL-5 has been documented to support metastasis by regulating a variety of host cell types, including eosinophils, regulatory T cells, natural killer cells (NK cells), macrophages, and neutrophils (*9*, *29*), we next determined the link between increased bone metastasis and eosinophils. For this, we crossed *Il-5* Tg mice with Eos-null mice (*Il-5* Tg and Eos-null mice) to eliminate eosinophils. Then, we reconstituted irradiated WT mice with BM from WT, *Il-5* Tg, or *Il-5* Tg and Eos-null mice to exclude the contribution of BM stromal cells to bone metastasis (Fig. 2F). Following tumor cell injection, the chimeric mice that received BM from *Il-5* Tg and Eos-null donor did not show an increase in metastasis numbers and tumor burden (Fig. 2, G to I). These results confirm that eosinophilia is indispensable for increased bone metastasis in *Il-5* Tg mice.

Eosinophils directly support tumor cell migration and metastasis formation

Given our observation that early stages of bone metastasis are enhanced in *Il-5* Tg mice (fig. S2D), we investigated whether eosinophils could directly promote tumor cell survival and growth. By conducting in vitro experiments, in which tumor cells were incubated in the absence (Control) or presence of eosinophils (+Eos) (fig. S3, A and B), we found no obvious alterations in the clonogenic activity of tumor cells (fig. S3C). Considering that eosinophils might induce apoptosis and necrosis of tumor cells as reported (*4*), we evaluated the survival of tumor cells cocultured with eosinophils. Unexpectedly, no significant effect on tumor cell death was found in the presence of eosinophils (fig. S3D). Similar findings revealed that there was neither an obvious difference in the proportion of 5-ethynyl-2′-deoxyuridine (EdU)–positive proliferating tumor cells (fig. S3E) nor a change in the cell cycle of tumor cells (fig. S3F) with or without eosinophils. These results implicate that eosinophils have no substantial effect on altering tumor cell growth.

We subsequently performed a migration assay in vitro. The ability of tumor cell migration was significantly enhanced upon direct or indirect contact with eosinophils in culture, suggesting that eosinophils promote tumor cell migration via a contact-independent manner (Fig. 3, A and B). We probed the results in the migration assays with the BM supernatant from *Il-5* Tg mice and their littermate

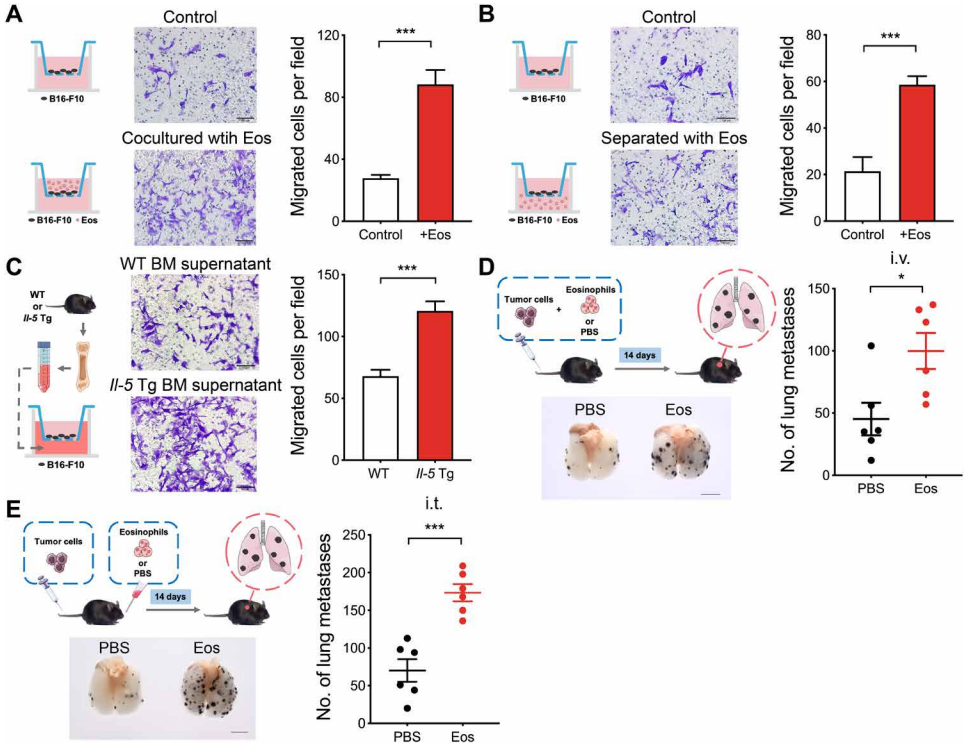

Fig. 3. Eosinophils promote tumor cell migration and metastasis formation. (**A**) Schematic diagram, representative crystal violet staining, and quantification of migrated B16-F10 cells cocultured with eosinophils. (**B**) Schematic diagram, representative crystal violet staining, and quantification of migrated B16-F10 cells toward eosinophils in the lower compartment. (**C**) Schematic diagram, representative crystal violet staining, and quantification of migrated B16-F10 cells toward BM supernatants from WT or *Il-5* Tg mice. (**D**) Comparison of the metastatic foci in the lung on day 14. Mice were injected with tumor cells and eosinophils (Eos) or only tumor cells (PBS) intravenously (i.v.). (**E**) Comparison of the metastatic foci in the lung on day 14. Mice were injected with tumor cells (intravenously) and immediately transferred of eosinophils or PBS [intratracheally (i.t.)] into the lung. (D) and (E) show the representative photograph and quantification of lung metastasis on day 14, $n = 6$ mice per group. Statistical analyses were performed by Student's *t* test (A to E). Data are presented as mean ± SEM from one representative experiment of three independent experiments. $^{*}P < 0.05$ and $^{***}P < 0.001$.

controls (Fig. 3C), demonstrating that eosinophil-derived factors could potentially promote tumor cell migration. Consistent with results in mice, human tumor cell lines were also found to migrate toward human eosinophils (fig. S4), indicating a translational value of the finding.

Then, the direct contribution of eosinophils to metastasis formation was assessed by using adoptive transfer techniques in vivo (fig. S5). We mixed tumor cells with eosinophils and then intravenously co-injected the mixture into WT mice, which resulted in increased lung metastasis compared to tumor cell injection alone (Fig. 3D). In parallel experiments, eosinophils were adoptively transferred (intratracheally) immediately following tumor cell intravenous injection, which resulted in similar consequences (Fig. 3E). Moreover, eosinophils were more potent in promoting lung metastasis when intratracheally transferred before intravenous tumor cell injection (fig. S6). We further characterized immune cell populations in the metastatic microenvironment at 24 hours after transfer of eosinophils. There were no significant changes in the number of alveolar macrophages, $CD4^+$ T and $CD8^+$ T lymphocytes, NK cells, dendritic cells (DCs), neutrophils, or monocytes, except increased eosinophils (fig. S7), suggesting that the increased metastasis was mainly due to the direct effect of eosinophils on tumor cells. Together, these results show that eosinophils are sufficient to support tumor cell migration and metastasis formation directly.

We next looked into the relationship between eosinophils and metastasis in patients with cancer. Malignant pleural effusion (MPE) of patients with pleural metastasis was detected with more eosinophils relative to pleural effusions from non–cancer patients (Fig. 4, A and B), without changes in other immune cells, including macrophages, lymphocytes, and neutrophils (fig. S8).

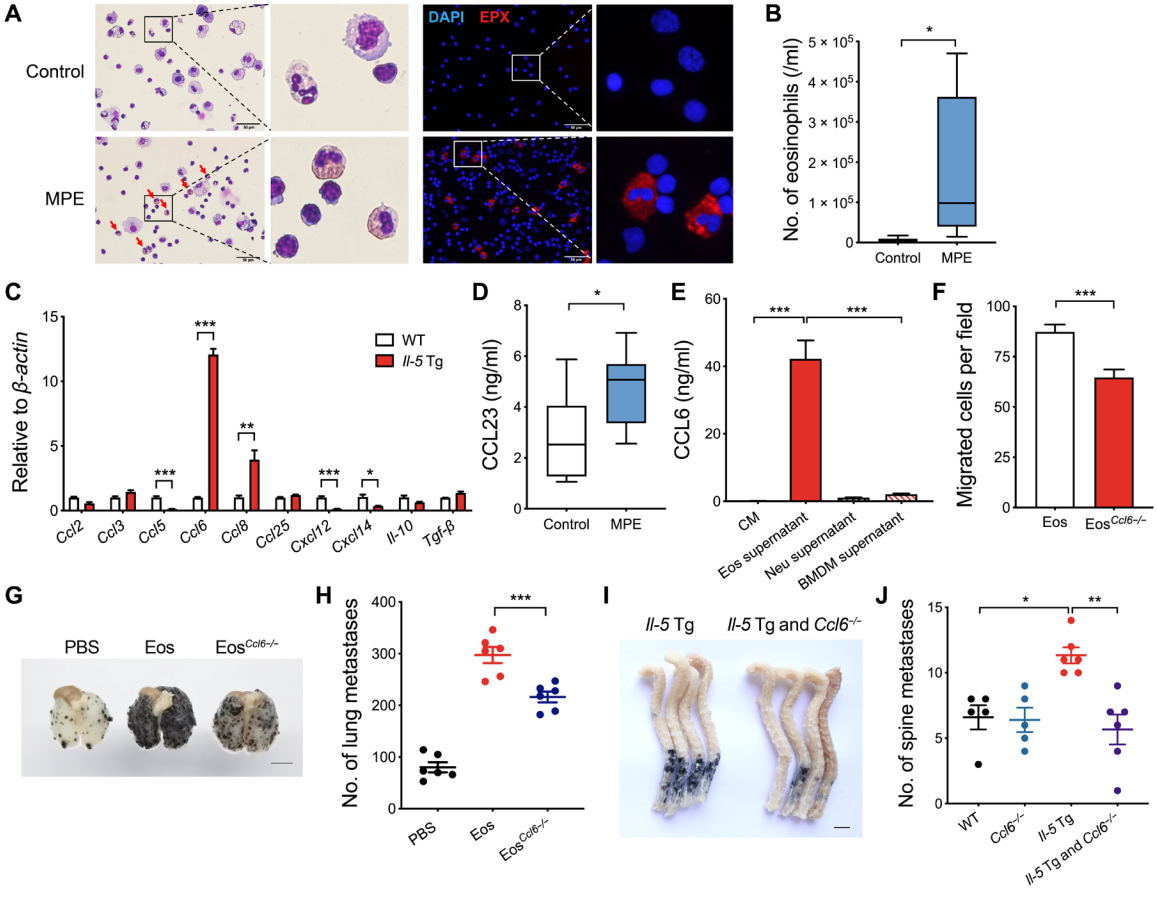

Fig. 4. CCL6 mediates eosinophil-induced tumor cell migration and metastasis formation. (**A**) Representative images of control pleural effusion cells from non–cancer patients and MPE cells from patients with cancer with pleural metastasis. The left panel is Wright-Giemsa staining. Scale bars, 50 μm. Arrows, eosinophils. The right panel is EPX staining. (**B**) The number of eosinophils in control pleural effusion ($n = 8$) and MPE ($n = 8$) by flow cytometry analysis. (**C**) The ratio of a panel of cytokine and chemokine mRNA in WT BM cells versus *Il-5* Tg BM cells, as assayed by RT-qPCR. (**D**) The protein levels of CCL23 in pleural fluid from patients with pleural metastasis ($n = 8$) and non–cancer patients ($n = 8$). (**E**) The protein levels of CCL6 in control medium (CM), the culture supernatant from eosinophils (Eos), neutrophils (Neu), and bone marrow–derived macrophages (BMDM). (**F**) The number of migrated B16-F10 cells per field toward CCL6-sufficient eosinophils (Eos, isolated from *Il-5* Tg mice) or CCL6-deficient eosinophils ($Eos^{Ccl6-/-}$, isolated from *Il-5* Tg and $Ccl6^{-/-}$ mice). (**G** and **H**) Representative photograph and quantification of metastatic foci in lungs on day 14. WT mice were injected with B16-F10 cells (intravenously) and transferred with Eos or $Eos^{Ccl6-/-}$ (intratracheally). Scale bar, 5 mm. (**I** and **J**) Representative photograph and quantification of metastatic foci in the spine on day 14. WT, $Ccl6^{-/-}$, *Il-5* Tg, and *Il-5* Tg and $Ccl6^{-/-}$ mice were injected with B16-F10 cells via caudal arteries. Scale bar, 5 mm. (H and J) $n = 5$ to 6 mice per group. Statistical analyses were performed by Student's *t* test (B to F) and one-way ANOVA (H to J). Data are presented as mean ± SEM from one representative experiment of three independent experiments (C, E, F, H, and J) or represented as box; the whiskers indicate Tukey (B and D). $^*P < 0.05$, $^{**}P < 0.01$, and $^{***}P < 0.001$.

CCL6 is essential for eosinophil-induced tumor cell migration and eosinophilia-dependent metastasis formation

We aimed to identify the effective factor of eosinophils promoting tumor cell migration and metastasis formation. Previous studies have reported that cytokines and chemokines, including CCL2 (*30*), CCL3 (*31*), CCL5 (*20*), CCL6 (*15*), CCL8 (*32*), CXCL12 (*33*), and CXCL14 (*34*), directly or indirectly target tumor cells to promote metastasis. We performed real-time quantitative polymerase chain reaction (RT-qPCR) to screen a panel of cytokines and chemokines in BM cells from *Il-5* Tg mice and WT mice. CCL6 was the most abundantly measured cytokine in *Il-5* Tg mice (Fig. 4C). The expression of CCL6 in BM cells was further examined by immunofluorescence (fig. S9A). As CCL23 has been identified as the human ortholog of murine CCL6, we subsequently assessed the level of CCL23 in human samples and found an increased CCL23 concentration in MPE relative to pleural effusions from non–cancer patients (Fig. 4D). Furthermore, high secretion of CCL6 was mainly identified in eosinophils (Fig. 4E). Similarly, CCL23 expressed in human eosinophils was validated in human blood and MPE cells (fig. S9B). Also, the expression of CCL23 is positively correlated with the number of eosinophils in human pleural effusion samples (fig. S9C).

To ascertain whether eosinophil-derived CCL6 was involved in tumor cell migration and metastasis, we generated *Ccl6* knockout mice ($Ccl6^{-/-}$) and crossed them with *Il-5* Tg mice (*Il-5* Tg and $Ccl6^{-/-}$). The basal number of eosinophils did not differ in *Il-5* Tg and $Ccl6^{-/-}$ mice relative to *Il-5* Tg mice (fig. S10, A and B). Two types of eosinophils (Eos from *Il-5* Tg mice and $Eos^{Ccl6-/-}$ from *Il-5* Tg and $Ccl6^{-/-}$ mice) were isolated to perform migration assays in vitro. Notably, the number of migrated tumor cells toward $Eos^{Ccl6-/-}$ was reduced (Fig. 4F). Loss of eosinophils or CCL6 did not affect the baseline lung metastasis in vivo (fig. S10, C and D), whereas CCL6 deficiency in eosinophils significantly reduced the eosinophilia-dependent lung metastasis (Fig. 4, G and H, and fig. S10E). *Il-5* Tg and $Ccl6^{-/-}$ mice also displayed much fewer bone metastases following tumor cell injection via caudal arteries relative to *Il-5* Tg mice (Fig. 4, I and J). Moreover, following intravenous tumor cell injection, the increased metastasis numbers and the tumor burden in bones were both reduced in *Il-5* Tg mice with CCL6 deficiency (fig. S11). Overall, these observations reveal that CCL6 is essential for eosinophil-induced tumor cell migration and eosinophilia-dependent metastasis formation in vivo.

Inhibition of CCL6 receptor CCR1 alleviates tumor cell migration and metastasis formation

CCR1 has been reported to be a putative CCL6 receptor (*35*). We explored whether eosinophil-derived CCL6 could recruit tumor cells to the metastatic sites through CCR1. We performed stable knockdown of CCR1 in B16-F10 cells by lentivirus short hairpin–mediated RNA (shRNA), with lentivirus-nontargeting shRNA as control (fig. S12A). Migration of CCR1-deficient B16-F10 (shCCR1 B16-F10) cells toward eosinophils or eosinophil culture supernatant was significantly decreased (Fig. 5A and fig. S12B). CCR1-deficient B16-F10 cells also displayed fewer bone metastases in *Il-5* Tg mice and fewer lung metastases in OVA-challenged mice (Fig. 5, B and C). These results provide evidence that the expression of CCR1 in tumor cells is critical for eosinophil-induced tumor cell migration and metastasis formation.

We further examined the effects of CCR1 inhibition on tumor cells by using CCR1-specific inhibitor BX471. BX471 significantly attenuated the migration of B16-F10 cells induced by eosinophil supernatant in vitro (Fig. 5, D and E). BX471-treated tumor cells developed significantly fewer bone metastases in vivo (Fig. 5, F and G). As CCL6 deficiency in eosinophils or CCR1 inhibition in tumor cells is sufficient to relieve eosinophil-induced tumor cell migration and metastasis formation, CCL6-CCR1 signaling could be a valuable therapeutic strategy for preventing eosinophilia-dependent tumor metastasis (Fig. 5H).

DISCUSSION

Eosinophils represent a minor subset of granulocytes that infiltrated in human cancers and several murine tumors. Accumulating evidence suggests their role in the orchestration of antitumor responses (*5*, *6*, *36*, *37*). However, here our study has uncovered an unfavorable role of eosinophilic inflammation in tumor metastasis. Eosinophils promote the migration of tumor cells without altering tumor cell survival, and eosinophilia is responsible for the establishment of bone metastasis in eosinophil-enriched mice. Mechanistic investigations revealed that eosinophils primarily secrete CCL6 to recruit tumor cells to their local sites through CCR1. Our results confirmed that blocking CCL6-CCR1 signaling is sufficient to relieve eosinophil-induced tumor cell migration and eosinophilia-dependent tumor metastasis.

A key finding of our study is an easily overlooked role of local eosinophilia contributing to metastasis. DEX relieves airway inflammation to block the eosinophilia-dependent lung metastasis. Notably, eosinophilia in the context of airway inflammation is accompanied by other factors, of which $CD4^+$ T cell activities might contribute to metastasis (*38*). Eosinophil deficiency abolished the $CD4^+$ T cell activation and proliferation in OVA-challenged mice, suggesting that eosinophils play an indispensable role in asthmatic airway inflammation (*39*). Consistently, eosinophil deficiency both relieves T helper 2-dominated airway inflammation (*24*) and reduces airway inflammation-dependent lung metastasis. However, eosinophil deficiency fails to relieve T helper 1–biased colonic inflammation (*25*) or colonic inflammation-dependent metastasis and even leads to primary tumor development (*6*).

In contrast with a previous study (*40*), we found that eosinophils fail to promote tumor cell death and instead contribute to tumor cell migration in vitro. Intravenous injection or intratracheal installation of eosinophils was shown to directly support the lung metastases, which is also in line with the results in vitro. The possible explanation is that the acquirement of cytotoxic activity in eosinophils against primary tumor depends on the specific stimuli (e.g., interferon-γ and IL-33) in the tumor microenvironment (*5*, *6*). Different stimuli could polarize eosinophils into distinct populations with opposing effects (*41*, *42*), which either control tumor growth or promote metastasis. In the present study, we propose that both allergic factor–activated eosinophils and nonactivated eosinophils will directly promote tumor cell migration and metastasis formation. Our findings could help to understand the contradictory role of eosinophils in the prognosis of patients with cancer.

Immune cells express a large number of receptors in addition to cytokines and chemokines, which can directly promote tumor cell migration and metastasis (*43*). In a previous study, overexpression of CCL6 accelerated tumor growth and enhanced local and metastasis spread (*15*). Similarly, our previous work found that eosinophils secrete CCL6 to promote hematopoietic stem cell proliferation

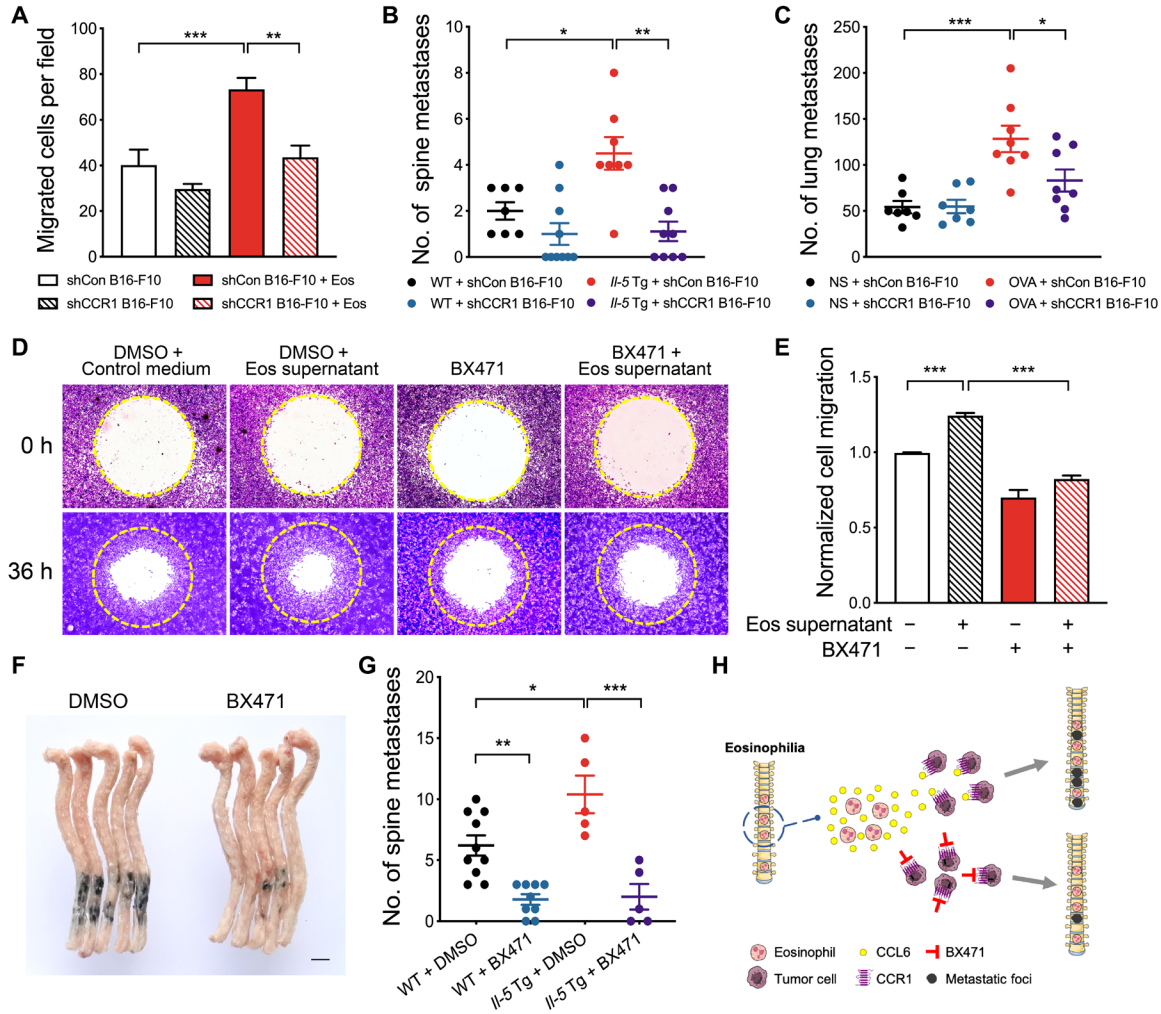

Fig. 5. CCR1 is required for eosinophilia-dependent metastasis. (**A**) The number of migrated CCR1-deficient B16-F10 cells (shCCR1 B16-F10) and CCR1-sufficient B16-F10 cells (shCon B16-F10) from the upper compartment toward eosinophils in the lower compartment of the Transwell system. (**B**) The number of metastatic foci in the spine on day 14. WT and *Il-5* Tg mice were injected with CCR1-deficient B16-F10 cells or CCR1-sufficient B16-F10 cells via caudal arteries, $n = 7$ to 10 mice per group. (**C**) The number of lung metastatic foci on day 42 according to Fig. 1A. NS or OVA-challenged WT mice were injected with CCR1-deficient B16-F10 cells or control B16-F10 cells (intravenously), $n = 7$ to 8 mice per group. (**D** and **E**) Representative crystal violet staining and quantification of migrated B16-F10 cells in the Oris cell migration assay. B16-F10 cells were cultured in control medium or eosinophil culture supernatant after migration for 36 hours treated with or without 20 μM BX471. (**F**) Representative photograph of metastasis foci in the spine of *Il-5* Tg mice injected with DMSO or BX471 pretreated tumor cells via caudal arteries. Scale bar, 5 mm. (**G**) Quantification of metastasis foci in the spine of WT and *Il-5* Tg mice after injection of DMSO or BX471 pretreated tumor cells via caudal arteries. WT, $n = 9$ to 10 mice per group; *Il-5* Tg, $n = 5$ mice per group. (**H**) Schematic representation of the proposed mechanism underlying eosinophilia-dependent metastasis. Statistical analyses were performed by one-way ANOVA (B and D). Data are presented as mean ± SEM from one representative experiment of three independent experiments. $^*P < 0.05$, $^{**}P < 0.01$, and $^{***}P < 0.001$.

and migration during eosinophilic inflammation (*14*). Here, we found a dominating role of CCL6 in the cross-talk between eosinophils and tumor cells, strengthening the idea that eosinophil-derived CCL6 directly supports the recruitment of tumor cells, thus promoting tumor metastasis. The evidence highlights the critical roles of chemokine networks in malignant progression. Nevertheless, few eosinophils reside in the lung under physiological conditions, as shown by the EPX immunohistochemistry analysis in tissues of control mice. Therefore, baseline eosinophils or CCL6 may not lead to a significant effect on metastasis. CCL23 shares structural homology with CCL6 and is reported to play similar promoting roles in cancer metastasis (*18*). In our study, we observed increased eosinophils and elevated expression of CCL23 in MPE. Further studies based on clinical data are required to determine the causal relationship between high expression of CCL23 and risk of cancer metastasis. Also, the chemokine receptors expressed in tumor cells should not be ignored. We found that inhibiting CCR1 in tumor cells results in decreased tumor metastasis in both WT mice and eosinophil-enriched mice, which provide a rationale for the application of CCR1 inhibitors in treating metastatic disease.

In addition to the eosinophil–tumor cell interactions in metastasis, the functional modulatory role of eosinophils that cross-talk with $CD8^+$ T cells in cancer immunity was previously appreciated (*37*). Here, our results show that intratracheally adoptive transfer of eosinophils promotes lung metastasis without causing obvious changes in the number of $CD8^+$ T cells in the lung, suggesting that

the increased metastasis mainly depends on the direct cross-talk between eosinophils and tumor cells rather than additional indirect effects by T cells. Thus, the clinical study should consider whether a direct causal relationship exists between infiltration of eosinophils into tumors and simultaneous antitumor T cell response. Also, clinical cancer immunotherapy to enhance infiltration of eosinophils into the tumor might be an invalid approach to recruiting T cells to kill tumor cells and might even worsen the prognosis in patients with cancer.

On the basis of the current findings and the above discussion, more attention should be paid to evaluate the metastasis-associated tissue eosinophilia in patients with cancer. Here, we predicted that directly targeting inflammation with eosinophil infiltration or blocking the eosinophil-related chemokine pathway could achieve clinical benefits in patients with cancer. We also call for caution an increased risk of metastasis and a poor prognosis induced by eosinophilia in patients with cancer. Last, we have identified a previously unknown CCL6-dependent prometastatic activity of eosinophils in supporting tumor cell recruitment, which can be targeted by a CCR1 inhibitor and might represent an approach to preventing metastatic disease.

MATERIALS AND METHODS

Cell culture

The murine B16-F10 cell line was a gift given by J. Q. Gao (Institute of Pharmaceutics, College of Pharmaceutical Sciences, Zhejiang University, China). B16-F10 cells were cultured in Dulbecco's minimum essential medium with 10% fetal bovine serum (FBS) in 5% CO_2 at 37°C. Cell viability was 95%, as assessed by Trypan Blue exclusion.

Mice

Il-5 Tg mice and *epo*-DT transgenic (Eos-null) mice were a gift from J. J. Lee (Department of Biochemistry and Molecular Biology, Mayo Clinic, USA). *Ccl6* knockout mice were generated in Nanjing Biomedical Research Institute of Nanjing University. *Il-5* Tg and Eos-null mice were generated by crossing *Il-5* Tg and Eos-null mice, which have been backcrossed to C57BL/6 purchased from Shanghai SLAC Laboratory Animal Co., Ltd. for over 20 generations and maintained in a specific pathogen–free facility in the animal center at Zhejiang University. All mice used for the experiment were at 8 weeks of age. The genotype $Ccl6^{-/-}$, *Il-5* Tg mice, Eos-null, and their WT littermates were confirmed by PCR analysis. All the animal experiments were strictly conducted in accordance with the protocols approved by the Ethics Committee for Animal Studies at Zhejiang University, China.

OVA-sensitized and -challenged asthma model

The airway inflammation was analyzed using an OVA sensitization and OVA-challenged asthma model. Briefly, asthmatic mice were sensitized by an intraperitoneal injection with 200 μl of 80 μg of grade V chicken egg OVA (Sigma-Aldrich) emulsified in 2.25 mg of Imject Alum Adjuvant (Thermo Fisher Scientific) on days 0 and 14. Control mice were injected with the same volume of normal saline (NS) instead. On days 24 to 28, mice were subsequently challenged with an aerosol generated from 1.5% OVA in saline or NS alone for 40 min by an ultrasonic atomizer (OMRON). For the DEX treatment experiment, mice have received DEX (Sigma-Aldrich) at 2 mg/kg in phosphate-buffered saline (PBS) administered intraperitoneally 1 hour after each OVA aerosol challenge. Mice were euthanized at 6 hours after the fourth OVA challenge on day 27. Then, lung tissues were harvested to assess eosinophilic inflammation by flow cytometry, histology, and immunohistochemistry. For the further establishment of the lung metastasis model, B16-F10 mouse melanoma cells (5×10^5 suspended in 200 μl of PBS) were intravenously injected 18 hours before the last OVA challenge on day 27, and mice were euthanized on day 42 (Fig. 1A).

DSS-induced colitis model

Colitis was induced by administering DSS [2% (w/v)] 36,000 to 50,000 kDa (MP Biomedicals) to 8-week-old mice for up to 7 days. On day 8, mice were used to establish the metastasis model with tumor cells or euthanized to harvest the colons for assessing eosinophilic inflammation by flow cytometry, histology, and immunohistochemistry.

Experimental metastasis assay

For experimental lung metastasis models, B16-F10 mouse melanoma cells (5×10^5 suspended in 200 μl of PBS) were injected into the tail vein. For experimental colon metastasis models, B16-F10 mouse melanoma cells (5×10^5 suspended in 200 μl of PBS) were injected into the abdominal cavities. For experimental bone metastasis models, B16-F10 mouse melanoma cells (5×10^5 suspended in 100 μl of PBS) were injected into the caudal artery of anesthetized mice using a 29 G syringe needle in a short time (<3 s) for bone metastasis analysis. Mice were euthanized on day 14 after tumor cell injection. Lungs and bones (spine, femur, and tibia) from B16-F10–bearing mice were harvested and fixed in formalin fixative solution for 24 hours and surface tumors were counted. Colon from B16-F10–bearing mice was harvested and surface tumors were counted. Tumor burden per bone was defined as the area of spine bone occupied by cancer cells (*44*), which was microscopically measured on hematoxylin and eosin–stained slides of the spine at 4 × 10 magnification.

Transwell migration assay

Migration experiments were performed using 8-μm Transwell cell culture inserts (Corning) in 24-well plates. The upper compartment was added with 200 μl of medium containing eosinophils (5×10^5) and tumor cells (5×10^4), and the lower compartment was added with 600 μl of medium containing 10% FBS. Cells were attached and migrated for 24 to 48 hours. For the detached migration assay, tumor cells were placed into the upper compartment, and the lower compartment was added with 600 μl of medium containing 10% FBS with eosinophils (5×10^5) or eosinophil culture supernatant. The plates were cultured for 24 to 48 hours. The tumor cells on the upper surface of the Transwell chamber were removed carefully with a cotton swab, and those on the lower surface were fixed with methanol for 10 min, stained with 0.1% crystal violet for 15 min, and photographed. Cell migration was microscopically assessed by counting stained cells visually at 20 × 10 magnification.

Oris cell migration assay

Cells were plated at a concentration of 1×10^5/ml and then were seeded on fibronectin (5 μg/ml; Sigma-Aldrich)–coated 96-well plates fitted with stoppers (Platypus Technologies, CMA1.101). Cells were incubated overnight in a humidified chamber at 37°C and 5% CO_2 before the removal of stoppers. For analysis of cell migration following inhibition of CCR1, cells were incubated with dimethyl sulfoxide (DMSO) (control), BX471 (20 μM, MedChemExpress), eosinophil

supernatant with DMSO, or eosinophil supernatant with BX471 for 36 hours after stopper removal. Cells were fixed with methanol for 10 min, stained with 0.1% crystal violet for 15 min, and photographed. In the duplicate quantitative test, cells were fixed and stained with 4′,6-diamidino-2-phenylindole. Fluorescent images were taken at 0 and 36 hours upon removal of stoppers, and cell migration was quantified by using ImageJ as outlined.

Real-time quantitative PCR

Total RNA was extracted from BM cells with Trizol reagent (Takara), and the quality of RNA was assessed with the NanoDrop2000 Spectrophotometer (Thermo Fisher Scientific) according to the manufacturer's instructions. mRNA was reverse-transcribed using a PrimeScript RT-PCR kit (Takara) and cDNA was subjected to RT-qPCR with SYBR Premix Ex Taq (Perfect Real Time; Takara). The PCR primers were purchased from Shanghai Sangon (Shanghai, China). RT-qPCR cycling was carried out on a 7500 Real-Time PCR System (Applied Biosystems). The mRNA levels were calculated using the comparative parameter threshold cycle (Ct) and normalized to β-actin. The sequences of primers used were as follows:

β-actin: forward, 5′-CCACTGCCGCATCCTCTTCCT-3′; reverse, 5′-CACACAGAGTACTTGCGCTCAGG-3′; *Tgfβ*: forward, 5′-CTTCAGCTCCACAGAGAAGA-3′; reverse, 5′-CTTCAGCTCCACAGAGAAGA-3′; *Il-10*: forward, 5′-CTTACTGACTGGCATGAGGATCA-3′; reverse, 5′-GCAGCTCTAGGAGCATGTGG-3′; *Ccl5*: forward, 5′-GCTGCTTTGCCTACCTCTCC-3′; reverse, 5′-TCGAGTGACAAACACGACTGC-3′; *Ccl6*: forward, 5′-AAGAAGATCGTCGCTATAACCCT-3′; reverse, 5′ GCTTAGGCACCTCTGAACTCTC-3′; *Ccl2*: forward, 5′-AGGTCCCTGTCATGCTTCTG-3′; reverse, 5′-TCTGGACCCATTCCTTCTTG-3′; *Ccl8*: forward, 5′-TCTACGCAGTGCTTCTTTGCC-3′; reverse, 5′-AAGGGGGATCTTCAGCTTTAGTA-3′; *Ccl3*: forward, 5′-TGTACCATGACACTCTGCAAC-3′; reverse, 5′-CAACGATGAATTGGCGTGGAA-3′; *Ccl25*: forward, 5′-GACTGCTGCCTGGGTTACC-3′; reverse, 5′-TGGCGGAAGTAGAATCTCACA-3′; *Cxcl12*: forward, 5′-TGCATCAGTGACGGTAAACCA-3′; reverse, 5′-CACAGTTTGGAGTGTTGAGGAT-3′; and *Cxcl14*: forward, 5′-AGTGTAAGTGTTCCCGGAAGG-3′; reverse, 5′-GCAGTGTGGGTACTTTGGCTT-3′.

Human pleural effusions

Human pleural effusions were obtained during initial diagnostic thoracenteses at the Respiratory Department of the Second Affiliated Hospital of the Zhejiang University School of Medicine. Cells in pleural effusions were counted, centrifuged, and lysed. Then, eosinophils were determined by visual examination of Wright-Giemsa staining, immunofluorescence analysis with EPX staining, and flow cytometry analysis. The study protocol was approved by the Ethics Committee of the Second Affiliated Hospital, Zhejiang University School of Medicine. All the patients provided written informed consent and understood that their tissues would be used for research.

ELISA analysis

Eosinophils isolated from *Il-5* Tg mice, neutrophils isolated by Ly6G positive selection from WT BM cells, and bone marrow–derived macrophages (BMDMs) induced by macrophage colony-stimulating factor (20 ng/ml) administration for 5 days were cultured at a concentration of 5×10^6/ml with complete medium for 6 hours to collect culture supernatant. CCL6 levels in the supernatant were then measured using the Mouse CCL-6/C-C Motif Chemokine 6 ELISA (enzyme-linked immunosorbent assay) Kit (Thermo Fisher Scientific). CCL23 levels in human pleural effusions are measured using the Human C-C Motif Chemokine 23 ELISA Kit (Thermo Fisher Scientific), and experiments were performed according to the manufacturer's instruction.

Statistical analysis

Data are mainly expressed as mean ± SEM. The unpaired two-tailed Student's *t* test was used for two groups, one-way analysis of variance (ANOVA) test was used for multiple groups, and Fisher's exact test was used for metastasis ratio. $P < 0.05$ was considered statistically significant. Statistical analyses were performed by Prism 6 (GraphPad 6).

SUPPLEMENTARY MATERIALS

Supplementary material for this article is available at http://advances.sciencemag.org/cgi/content/full/7/22/eabb5943/DC1

View/request a protocol for this paper from *Bio-protocol*.

REFERENCES AND NOTES

1. S. I. Grivennikov, F. R. Greten, M. Karin, Immunity, inflammation, and cancer. *Cell* **140**, 883–899 (2010).
2. M. C. Turner, Y. Chen, D. Krewski, P. Ghadirian, M. J. Thun, E. E. Calle, Cancer mortality among US men and women with asthma and hay fever. *Am. J. Epidemiol.* **162**, 212–221 (2005).
3. G. Varricchi, M. R. Galdiero, S. Loffredo, V. Lucarini, G. Marone, F. Mattei, G. Marone, G. Schiavoni, Eosinophils: The unsung heroes in cancer? *Onco. Targets. Ther.* **7**, e1393134 (2018).
4. S. Gatault, M. Delbeke, V. Driss, A. Sarazin, A. Dendooven, J. E. Kahn, G. Lefevre, M. Capron, IL-18 is involved in eosinophil-mediated tumoricidal activity against a colon carcinoma cell line by upregulating LFA-1 and ICAM-1. *J. Immunol.* **195**, 2483–2492 (2015).
5. C. Hollande, J. Boussier, J. Ziai, T. Nozawa, V. Bondet, W. Phung, B. Lu, D. Duffy, V. Paradis, V. Mallet, G. Eberl, W. Sandoval, J. M. Schartner, S. Pol, R. Barreira da Silva, M. L. Albert, Inhibition of the dipeptidyl peptidase DPP4 (CD26) reveals IL-33-dependent eosinophil-mediated control of tumor growth. *Nat. Immunol.* **20**, 257–264 (2019).
6. H. Reichman, M. Itan, P. Rozenberg, T. Yarmolovski, E. Brazowski, C. Varol, N. Gluck, S. Shapira, N. Arber, U. Qimron, D. Karo-Atar, J. J. Lee, A. Munitz, Activated eosinophils exert antitumorigenic activities in colorectal cancer. *Cancer Immunol. Res.* **7**, 388–400 (2019).
7. H. F. Rosenberg, K. D. Dyer, P. S. Foster, Eosinophils: Changing perspectives in health and disease. *Nat. Rev. Immunol.* **13**, 9–22 (2013).
8. S. Libreros, R. Garcia-Areas, P. Keating, N. Gazaniga, P. Robinson, A. Humbles, V. L. Iragavarapu-Charyulu, Allergen induced pulmonary inflammation enhances mammary tumor growth and metastasis: Role of CHI3L1. *J. Leukoc. Biol.* **97**, 929–940 (2015).
9. M. Ikutani, T. Yanagibashi, M. Ogasawara, K. Tsuneyama, S. Yamamoto, Y. Hattori, T. Kouro, A. Itakura, Y. Nagai, S. Takaki, K. Takatsu, Identification of innate IL-5-producing cells and their role in lung eosinophil regulation and antitumor immunity. *J. Immunol.* **188**, 703–713 (2012).
10. R. Zaynagetdinov, T. P. Sherrill, L. A. Gleaves, A. G. McLoed, J. A. Saxon, A. C. Habermann, L. Connelly, D. Dulek, R. S. Peebles Jr., B. Fingleton, F. E. Yull, G. T. Stathopoulos, T. S. Blackwell, Interleukin-5 facilitates lung metastasis by modulating the immune microenvironment. *Cancer Res.* **75**, 1624–1634 (2015).
11. V. Panagopoulos, D. A. Leach, I. Zinonos, V. Ponomarev, G. Licari, V. Liapis, W. V. Ingman, P. Anderson, M. O. DeNichilo, A. Evdokiou, Inflammatory peroxidases promote breast cancer progression in mice via regulation of the tumour microenvironment. *Int. J. Oncol.* **50**, 1191–1200 (2017).
12. L. Ye, H. Wang, H. Li, H. Liu, T. Lv, Y. Song, F. Zhang, Eosinophil peroxidase over-expression predicts the clinical outcome of patients with primary lung adenocarcinoma. *J. Cancer* **10**, 1032–1038 (2019).
13. A. Orlofsky, E. Y. Lin, M. B. Prystowsky, Selective induction of the beta chemokine C10 by IL-4 in mouse macrophages. *J. Immunol.* **152**, 5084–5091 (1994).
14. C. Zhang, W. Yi, F. Li, X. Du, H. Wang, P. Wu, C. Peng, M. Luo, W. Hua, C. C. Wong, J. J. Lee, W. Li, Z. Chen, S. Ying, Z. Ju, H. Shen, Eosinophil-derived CCL-6 impairs hematopoietic stem cell homeostasis. *Cell Res.* **28**, 323–335 (2018).
15. F. Yi, R. Jaffe, E. V. Prochownik, The *CCL6* chemokine is differentially regulated by c-Myc and L-Myc, and promotes tumorigenesis and metastasis. *Cancer Res.* **63**, 2923–2932 (2003).

16. R. D. Berahovich, Z. Miao, Y. Wang, B. Premack, M. C. Howard, T. J. Schall, Proteolytic activation of alternative CCR1 ligands in inflammation. *J. Immunol.* **174**, 7341–7351 (2005).
17. H. Miyoshi, A. Morishita, J. Tani, T. Sakamoto, K. Fujita, A. Katsura, M. Tatsuta, T. Nomura, H. Yoneyama, H. Iwama, Y. Suzuki, T. Masaki, Expression profiles of 507 proteins from a biotin label-based antibody array in human colorectal cancer. *Oncol. Rep.* **31**, 1277–1281 (2014).
18. H. H. Yan, J. Jiang, Y. Pang, B. R. Achyut, M. Lizardo, X. Liang, K. Hunter, C. Khanna, C. Hollander, L. Yang, CCL9 induced by TGFβ signaling in myeloid cells enhances tumor cell survival in the premetastatic organ. *Cancer Res.* **75**, 5283–5298 (2015).
19. Y. Zhu, X. M. Gao, J. Yang, D. Xu, Y. Zhang, M. Lu, Z. Zhang, Y. Y. Sheng, J. H. Li, X. X. Yu, Y. Zheng, Q. Z. Dong, L. X. Qin, C-C chemokine receptor type 1 mediates osteopontin-promoted metastasis in hepatocellular carcinoma. *Cancer Sci.* **109**, 710–723 (2018).
20. K. Chen, Q. Liu, L. L. Tsang, Q. Ye, H. C. Chan, Y. Sun, X. Jiang, Human MSCs promotes colorectal cancer epithelial-mesenchymal transition and progression via CCL5/β-catenin/Slug pathway. *Cell Death Dis.* **8**, e2819 (2017).
21. B. Strilic, L. Yang, J. Albarran-Juarez, L. Wachsmuth, K. Han, U. C. Muller, M. Pasparakis, S. Offermanns, Tumour-cell-induced endothelial cell necroptosis via death receptor 6 promotes metastasis. *Nature* **536**, 215–218 (2016).
22. B. P. Tian, L. X. Xia, Z. Q. Bao, H. Zhang, Z. W. Xu, Y. Y. Mao, C. Cao, L. Q. Che, J. K. Liu, W. Li, Z. H. Chen, S. Ying, H. H. Shen, Bcl-2 inhibitors reduce steroid-insensitive airway inflammation. *J. Allergy Clin. Immunol.* **140**, 418–430 (2017).
23. A. Perales-Puchalt, N. Svoronos, D. O. Villarreal, U. Zankharia, E. Reuschel, K. Wojtak, K. K. Payne, E. K. Duperret, K. Muthumani, J. R. Conejo-Garcia, D. B. Weiner, IL-33 delays metastatic peritoneal cancer progression inducing an allergic microenvironment. *Onco. Targets. Ther.* **8**, e1515058 (2019).
24. J. J. Lee, D. Dimina, M. P. Macias, S. I. Ochkur, M. P. McGarry, K. R. O'Neill, C. Protheroe, R. Pero, T. Nguyen, S. A. Cormier, E. Lenkiewicz, D. Colbert, L. Rinaldi, S. J. Ackerman, C. G. Irvin, N. A. Lee, Defining a link with asthma in mice congenitally deficient in eosinophils. *Science* **305**, 1773–1776 (2004).
25. J. C. Masterson, E. N. McNamee, S. A. Fillon, L. Hosford, R. Harris, S. D. Fernando, P. Jedlicka, R. Iwamoto, E. Jacobsen, C. Protheroe, H. K. Eltzschig, S. P. Colgan, M. Arita, J. J. Lee, G. T. Furuta, Eosinophil-mediated signalling attenuates inflammatory responses in experimental colitis. *Gut* **64**, 1236–1247 (2015).
26. N. A. Lee, M. P. McGarry, K. A. Larson, M. A. Horton, A. B. Kristensen, J. J. Lee, Expression of IL-5 in thymocytes/T cells leads to the development of a massive eosinophilia, extramedullary eosinophilopoiesis, and unique histopathologies. *J. Immunol.* **158**, 1332–1344 (1997).
27. T. Kuchimaru, N. Kataoka, K. Nakagawa, T. Isozaki, H. Miyabara, M. Minegishi, T. Kadonosono, S. Kizaka-Kondoh, A reliable murine model of bone metastasis by injecting cancer cells through caudal arteries. *Nat. Commun.* **9**, 2981 (2018).
28. S. J. Bakewell, P. Nestor, S. Prasad, M. H. Tomasson, N. Dowland, M. Mehrotra, R. Scarborough, J. Kanter, K. Abe, D. Phillips, K. N. Weilbaecher, Platelet and osteoclast β_3 integrins are critical for bone metastasis. *Proc. Natl. Acad. Sci. U.S.A.* **100**, 14205–14210 (2003).
29. D. F. Quail, O. C. Olson, P. Bhardwaj, L. A. Walsh, L. Akkari, M. L. Quick, I. C. Chen, N. Wendel, N. Ben-Chetrit, J. Walker, P. R. Holt, A. J. Dannenberg, J. A. Joyce, Obesity alters the lung myeloid cell landscape to enhance breast cancer metastasis through IL5 and GM-CSF. *Nat. Cell Biol.* **19**, 974–987 (2017).
30. B. Z. Qian, J. Li, H. Zhang, T. Kitamura, J. Zhang, L. R. Campion, E. A. Kaiser, L. A. Snyder, J. W. Pollard, CCL2 recruits inflammatory monocytes to facilitate breast-tumour metastasis. *Nature* **475**, 222–225 (2011).
31. S. C. Robinson, K. A. Scott, F. R. Balkwill, Chemokine stimulation of monocyte matrix metalloproteinase-9 requires endogenous TNF-α. *Eur. J. Immunol.* **32**, 404–412 (2002).
32. E. Farmaki, I. Chatzistamou, V. Kaza, H. Kiaris, A CCL8 gradient drives breast cancer cell dissemination. *Oncogene* **35**, 6309–6318 (2016).
33. T. Murakami, W. Maki, A. R. Cardones, H. Fang, A. Tun Kyi, F. O. Nestle, S. T. Hwang, Expression of CXC chemokine receptor-4 enhances the pulmonary metastatic potential of murine B16 melanoma cells. *Cancer Res.* **62**, 7328–7334 (2002).
34. H. Pelicano, W. Lu, Y. Zhou, W. Zhang, Z. Chen, Y. Hu, P. Huang, Mitochondrial dysfunction and reactive oxygen species imbalance promote breast cancer cell motility through a CXCL14-mediated mechanism. *Cancer Res.* **69**, 2375–2383 (2009).
35. B. Ma, Z. Zhu, R. J. Homer, C. Gerard, R. Strieter, J. A. Elias, The C10/CCL6 chemokine and CCR1 play critical roles in the pathogenesis of IL-13-induced inflammation and remodeling. *J. Immunol.* **172**, 1872–1881 (2004).
36. V. Lucarini, G. Zicchedda, I. Macchia, V. La Sorsa, F. Peschiaroli, C. Buccione, A. Sistigu, M. Sanchez, S. Andreone, M. T. D'Urso, M. Spada, D. Macchia, C. Afferni, F. Mattei, G. Schiavoni, IL-33 restricts tumor growth and inhibits pulmonary metastasis in melanoma-bearing mice through eosinophils. *Oncoimmunology* **6**, e1317420 (2017).
37. R. Carretero, I. M. Sektioglu, N. Garbi, O. C. Salgado, P. Beckhove, G. J. Hammerling, Eosinophils orchestrate cancer rejection by normalizing tumor vessels and enhancing infiltration of $CD8^+$ T cells. *Nat. Immunol.* **16**, 609–617 (2015).
38. A. G. Taranova, D. Maldonado III, C. M. Vachon, E. A. Jacobsen, H. Abdala-Valencia, M. P. McGarry, S. I. Ochkur, C. A. Protheroe, A. Doyle, C. S. Grant, J. Cook-Mills, L. Birnbaumer, N. A. Lee, J. J. Lee, Allergic pulmonary inflammation promotes the recruitment of circulating tumor cells to the lung. *Cancer Res.* **68**, 8582–8589 (2008).
39. E. A. Jacobsen, K. R. Zellner, D. Colbert, N. A. Lee, J. J. Lee, Eosinophils regulate dendritic cells and Th2 pulmonary immune responses following allergen provocation. *J. Immunol.* **187**, 6059–6068 (2011).
40. F. Legrand, V. Driss, M. Delbeke, S. Loiseau, E. Hermann, D. Dombrowicz, M. Capron, Human eosinophils exert TNF-α and granzyme A-mediated tumoricidal activity toward colon carcinoma cells. *J. Immunol.* **185**, 7443–7451 (2010).
41. L. Y. Liu, M. E. Bates, N. N. Jarjour, W. W. Busse, P. J. Bertics, E. A. Kelly, Generation of Th1 and Th2 chemokines by human eosinophils: Evidence for a critical role of TNF-α. *J. Immunol.* **179**, 4840–4848 (2007).
42. C. Bouffi, M. Rochman, C. B. Zust, E. M. Stucke, A. Kartashov, P. C. Fulkerson, A. Barski, M. E. Rothenberg, IL-33 markedly activates murine eosinophils by an NF-κB–dependent mechanism differentially dependent upon an IL-4-driven autoinflammatory loop. *J. Immunol.* **191**, 4317–4325 (2013).
43. N. Nagarsheth, M. S. Wicha, W. Zou, Chemokines in the cancer microenvironment and their relevance in cancer immunotherapy. *Nat. Rev. Immunol.* **17**, 559–572 (2017).
44. P. Juárez, K. S. Mohammad, J. J. Yin, P. G. J. Fournier, R. C. McKenna, H. W. Davis, X. H. Peng, M. Niewolna, D. Javelaud, J. M. Chirgwin, A. Mauviel, T. A. Guise, Halofuginone inhibits the establishment and progression of melanoma bone metastases. *Cancer Res.* **72**, 6247–6256 (2012).

Acknowledgments: We are grateful to N. Lee and J. J. Lee for providing *Il-5* Tg and Eos-null mice. **Funding:** This work was supported by the National Natural Science Foundation of China (81930003, 81420108001, 81920108001, 81870007, and 81800024), the National Key R&D Program of China (2016YFA0100301), the Zhejiang Provincial Natural Science Foundation (LD19H160001), and the Major Research Plan (91642202). **Author contributions:** S.Y. and H.S. initiated the study and developed the concept of the paper. F. Li, X.D., F. Lan, and N.L. performed all experiments. C. Zhang, C. Zhu, X.W., Y.H., M.L., Z.S., and H.C. participated in animal experiments. C. Zhang, W.L., and Z.C. analyzed and interpreted the data. S.Y., H.S., F. Li, and C. Zhang wrote the manuscript. **Competing interests:** The authors declare that they have no competing interests. **Data and materials availability:** All data needed to evaluate the conclusions in the paper are present in the paper and/or the Supplementary Materials.

Submitted 5 March 2020
Accepted 8 April 2021
Published 26 May 2021
10.1126/sciadv.abb5943

Citation: F. Li, X. Du, F. Lan, N. Li, C. Zhang, C. Zhu, X. Wang, Y. He, Z. Shao, H. Chen, M. Luo, W. Li, Z. Chen, S. Ying, H. Shen, Eosinophilic inflammation promotes CCL6-dependent metastatic tumor growth. *Sci. Adv.* **7**, eabb5943 (2021).